ACS Medicinal Chemistry Letters

Letter

Structure-Guided Design of Novel, Potent and Selective Macrocyclic Plasma Kallikrein Inhibitors

Zhe Li, James Robert Partridge, Abel Silva-Garcia, Peter Rademacher, Andreas Betz, Qing Xu, Hing Leung Sham, YunJin Hu, Yuqing Shan, Bin Liu, Ying Zhang, Haijuan Shi, Qiong Xu, Xubo Ma, and Li Zhang

ACS Med. Chem. Lett., **Just Accepted Manuscript** • DOI: 10.1021/acsmedchemlett.6b00384 • Publication Date (Web): 06 Dec 2016

ACS Publications

ACS Medicinal Chemistry Letters is published by the American Chemical Society. 1155 Sixteenth Street N.W., Washington, DC 20036

Structure-Guided Design of Novel, Potent and Selective Macrocyclic Plasma Kallikrein Inhibitors

Zhe Li,[†,*] James Partridge,[†] Abel Silva-Garcia,[†] Peter Rademacher,[†] Andreas Betz,[†] Qing Xu,[†] Hing Sham,[†] Yunjin Hu,[‡] Yuqing Shan,[‡] Bin Liu,[‡] Ying Zhang,[‡] Haijuan Shi,[‡] Qiong Xu,[‡] Xubo Ma,[‡] Li Zhang[‡]

[†] Global Blood Therapeutics, South San Francisco, CA 94080

[‡] Pharmaron Xi'an Co., Xi'an, Shaanxi, China 710018

KEYWORDS: Hereditary angioedema, plasma kallikrein, protease inhibitor, structure-based design, macrocycle.

ABSTRACT: A series of macrocyclic analogs were designed and synthesized based on the co-crystal structure of small molecule plasma kallikrein (pKal) inhibitor, **2**, with the pKal protease domain. This led to the discovery of a potent macrocyclic pKal inhibitor **29**, with an IC_{50} of 2 nM for one olefinic isomer and 42.3 nM for the other olefinic isomer.

The serine protease plasma kallikrein (pKal) is a multifunctional enzyme involved in the early phase of intrinsic blood coagulation, kinin formation and fibrinolysis.[1] The native protease consists of a heavy chain, which mediates the interaction of pKal with other proteins, and the protease domain is located in the light chain. The two-domain structure of pKal results from the activation of its single chain precursor kallikrein (preKal) by the protease factor XIIa (FXIIa). In plasma the activation of preKal is triggered after autocatalytic conversion of FXII to FXIIa on surfaces and is accelerated by the cofactor high molecular weight kininogen (HMWK). The reaction is then amplified, by reciprocal activation of FXIIa by pKal. Under physiologic conditions FXII, HMWK and preKal form a complex with a variety of receptors and enzymes expressed on endothelial surfaces, which catalyzes the activation of pKal. After activation, pKal catalyzes the release of the proinflammatory peptide bradykinin from HMWK.[2] Further pKal appears to be involved in the generation of plasmin from plasminogen and renin from prorenin, which links the protease to fibrinolysis and the regulation of blood pressure. Because of the overlapping activities of pKal in clinically important processes, it appears to be a viable target for therapeutic intervention.[3]

In plasma the activity of pKal is mainly regulated by macrogobulin, antiplasmin and C1 esterase inhibitor (C1-INH). However, C1-INH appears to be the most important, since an inherited reduced expression or deficiency of the inhibitor results in excess release of bradykinin and leads to episodic swelling attacks in these patients termed hereditary angioedema (HAE). The frequency and severity of HAE attacks is highly variable and unpredictable. Some attacks of swelling that affect the larynx may block airway and can be fatal. Current treatment options for HAE patients are limited to biologics. These treatments, targeting to correct C1-INH deficiency, include replacement therapy either by plasma transfusion or infusion of recombinant C1-INH.[4] An engineered Kunitz-type protease inhibitor was also introduced for the treatment of HAE.[5] More recently, a monoclonal antibody against pKal has been evaluated in clinical trials and demonstrated early evidence of efficacy.[6]

A small molecule oral drug for prophylactic treatment of HAE is highly desirable. Only two small molecule non-peptidic pKal inhibitors are known, BCX4161 (**1**)[7] and compound **2** (Figure 1). BCX4161 and its backup compound BCX7353[8] are the only small molecule pKal inhibitors that have reached human clinical trials for HAE. Despite initial success in Phase 1b studies with HAE patients, BCX4161 failed in recent Phase 2 studies likely due to its poor PK profile and lack of adequate exposure and efficacy. The second generation compound BCX7353 (structure not reported) has also entered human trials recently.[8] A class of small molecules reported in patent literature[9] caught our attention. Many examples described in the application possess excellent potency against pKal. One compound (compound **2**,[9] Figure 1) was tested and found to have an

Figure 1. Literature small molecule inhibitors of pKal.

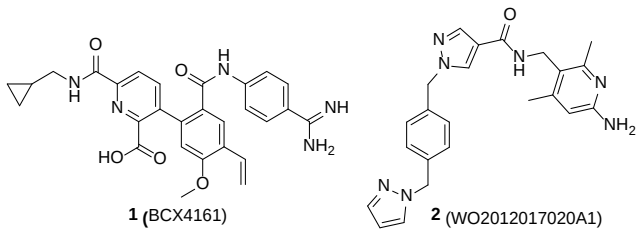

1 (BCX4161) **2** (WO2012017020A1)

enzymatic IC_{50} of 2.4 nM in our conditions. More importantly, the compound displayed excellent selectivity over a panel of eight closely related proteases. Subsequently, the compound was successfully co-crystallized with the purified protease domain of pKal and an X-ray structure was obtained (PDB code 5TZ9).[10] The inhibitor demonstrated a surprising mode of interaction, which upon binding resulted in a dramatic rearrange-

ment of amino acids surrounding the active site of pKal. Compound **2** binds to the active site of pKal and forces a rearrangement of Trp598 to expose a deep binding pocket. This allows the molecule to form critical stacking interactions with the catalytic histidine residue, His434, and two other residues: Trp598, and Tyr555. The lack of conservation in surrounding residues explains the >1,000-fold specificity over structurally similar proteases.

Compound **2** adopts a unique U-shape conformation that compliments the induced binding pockets of pKal. Several key interactions are visible and likely important for the binding potency. The middle pyrazole ring of **2** interacts with the imidazole ring of catalytic His434 via *pi-pi* stacking with an average distance of ~ 3.6 Å between them. The phenyl ring of **2** sits in a pocket surrounded by Ser597, Gly480 and Trp598. In addition to a *pi-pi* stacking interaction with Try555, the terminal pyrazole ring of **2** also forms water mediated interaction with the Pro-*R* hydrogen of CH_2 of Gly480 (Figures 2&3).

Figure 2. Co-crystal structure of pKal with **2**. Numbers in parenthesis represent the canonical chymotrypsin numbering scheme. Two water molecules are shown as blue spheres.

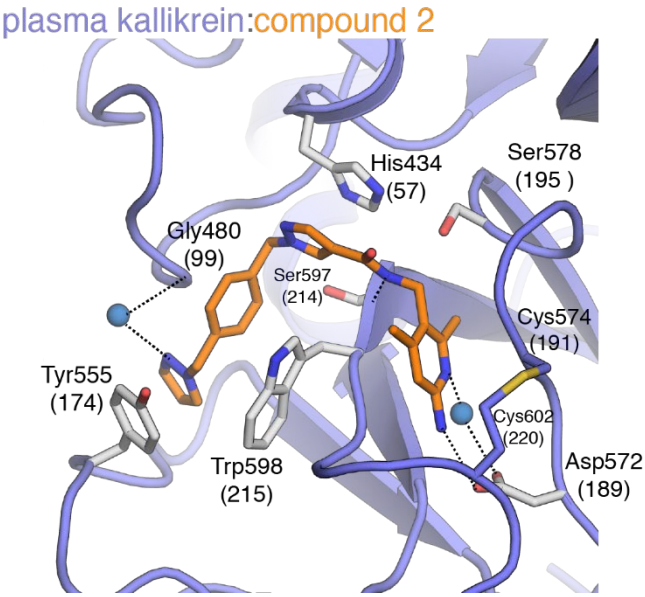

Figure 3. Schematic drawing generated by MOE showing key interactions between **2** and the active site residues of pKal.

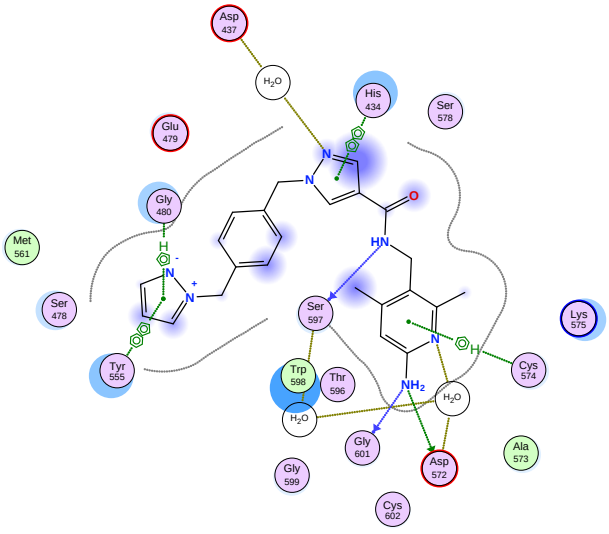

Compound **2** had little oral exposure when it was dosed in rats by oral gavage. After a 20 mg/kg dose, the C_{max} was 25 ng/mL and has a calculated oral bioavailability of ~6%. A possible explanation for the lack of oral exposure could be attributed to the physiochemical properties, mainly the presence of seven rotatable bonds which may have a negative impact on its permeability. Reducing the number of freely rotatable bonds by conformational restriction is a common medicinal chemistry approach to improve overall properties of lead compounds, such as selectivity,[11] potency,[12] and bioavailability.[13]

Figure 4. Co-crystal structure of **2** with yellow dots indicating linking points for macrocyclic analogs.

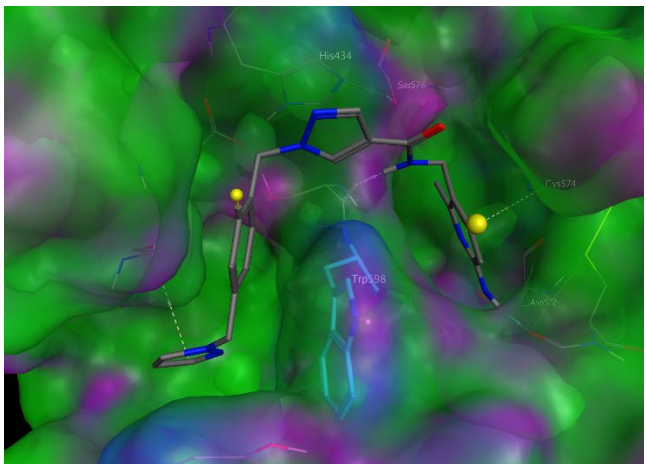

We sought to make rigidified analogs of **2** in hope to improve its oral bioavailability. Closer examination of the co-crystal structure of **2** with pKal revealed a possible way of modifying and restraining the molecule, namely, connecting the aminopyridine group, residing in the S1 pocket, to the phenyl group, residing near the S4 pocket, via a straight-chain alkyl linker that spans over the top of Trp598. As seen in the co-crystal structure, the space over Trp598 is open to solvents and has room to easily accommodate a straight-chain linker. Further analysis suggested that the best connecting points may be 2-methyl of the aminopyridine and 2-position of the phenyl ring (Figure 4).

Figure 5. Modeling of proposed macrocyclic **3** with an 8-atom trans-double bond linker.

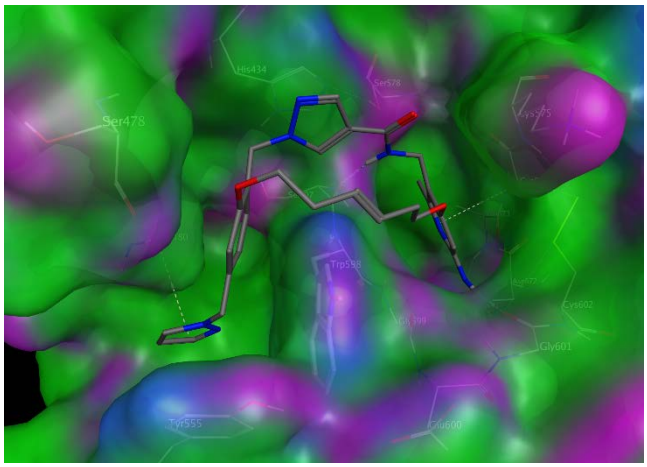

Computer modeling software MOE[14] was used to guide the design of the linker. Specifically, a potential linker alkyl chain was allowed to grow atom-by-atom from both the aminopyridine and the phenyl positions until the two half-chains met

in close proximity (< 2 Å) over the top of residue Trp598. The two half-chains were then connected with a single- or double-bond and the resulting macrocyclic structure was minimized (Amber10 EHT force field) within the binding pocket of pKal. For synthetic ease and accessibility, oxygen atoms were introduced at both ends of the linker as anchor points to the phenyl and aminopyridine rings, respectively. A double-bond in the middle of the linker may be advantageous in reducing the number of conformers associated a flexible alkyl chain linker. Our modeling suggested a six-atom straight-chain alkylene or alkenylene group with oxygen at both ends as the shortest possible linker. Based on modeling it seems that the -O$(CH_2)_6$O- or -O$(CH_2)_2$CH=CH$(CH_2)_2$O- linker adopts a favorable staggered *gauche-trans-gauche* conformation (Figure 5). Key interactions observed between 2 and pKal would be preserved in the proposed macrocyclic structure according to the model. These include the pi-pi stacking of pyrazole with His434; the hydrogen-bond between C=O of Ser597 and amide-NH of the macrocycle.

We sought to employ Grubbs ring-closing metathesis (RCM)[15-17] to synthesize the targeted macrocycle 3 (Figure 6). Macrocycle 3 or others with different ring sizes could be obtained directly from the key bis-alkene intermediates **4**-**6** via RCM reactions. These intermediates are derived from the corresponding acids (**7** and **8**) and amines (**9** and **10**).

Figure 6. Structure-based design of macrocycles.

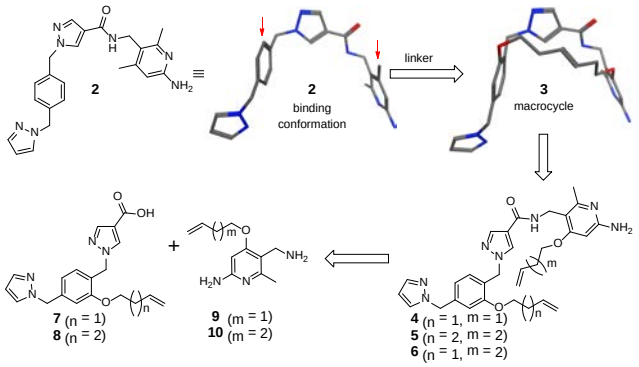

The *O*-alkenyl aminopyridines, **9** and **10**, were synthesized according to synthetic route outlined in Scheme 1. Condensation of 3-aminocrotononitrile **11** and 2-cyanoacetic acid **12** in the presence of acetic anhydride provided bis-nitrile **13**, which was treated with sodium ethoxide in ethanol to give 4-hydroxypyrdine intermediate **14** as its sodium salt. This intermediate was then *O*-alkylated with ω-alkyenyl bromides **15** and **16** followed by reduction with LAH to produce the desired *O*-alkenylated aminopyridine derivatives **9** and **10**, respectively.

Scheme 1. Synthesis of Intermediates 9 and 10[a]

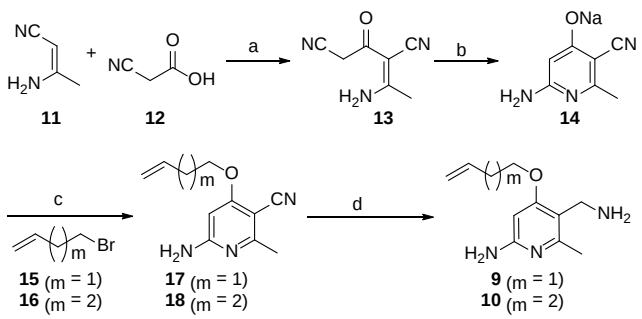

[a]Reagents and conditions: (a) Ac_2O, dioxane, reflux 2 h, 44%; (b) EtONa, EtOH, reflux, 89%; (c) for **17** K_2CO_3, 4-bromobut-1-ene (**15**), DMF 50 °C, 16 h, 74%; for **18** K_2CO_3, 5-bromopent-1-ene (**16**), DMF 50 °C, 16 h, 100%; (d) LAH, Et_2O, reflux, 16 h, 46% for **9** and 38% for **10**.

To synthesize the acid intermediate **7** (scheme 2), 2-hydroxy-4-methylbenzoic acid **19** with acetone under acidic conditions gave acetonide **20**. This was followed by benzylic bromination and displacement of the newly formed bromide **21** with pyrazole **22** to deliver **23**. Reduction of the ester and selective alkylation of the phenolic hydroxyl provided alkylated alcohol **25**, which was converted to the chloride **26** by reacting with thionyl chloride. *N*-alkylation with ethyl pyrazole-4-carboxylate **27**, followed by hydrolysis of the ethyl ester, provided the key acid intermediate **7** which was coupled with amine **9** to give bis-terminal alkene **4**. Ring-closing metathesis under standard conditions using Grubbs' II catalyst produced the macrocycle **3**.

Scheme 2. Synthesis of Macrocycles 3, 29, 30 and 31[a]

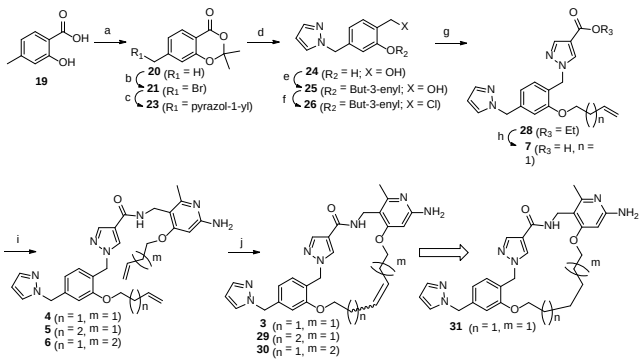

[a]Reagents and conditions: (a) TFAA,TFA, acetone, rt, 3 d, 46%; (b) NBS, BPO, CCl_4, 75 °C, 1 h, 66%; (c) pyrazole **22**, K_2CO_3, 50 °C, 2 h, 100%; (d) LAH, THF, -78 °C, 1 h, 84%; (e) **15**, Na_2CO_3, DMF, 80 °C, 14 h, 30%; (f) $SOCl_2$, DCM, rt, 30 min, 93%; (g) ethyl 1H-pyrazole-4-carboxylate **27**, K_2CO_3, DMF, rt, 14 h, 65%; (h)NaOH, MeOH/H_2O, rt, 85%; (i) **9** or **10**, HATU, DIPEA, DM, rt, 14 h, 63% for **4**; 59% for **5**; (j) Grubbs' catalyst (II), DCE, 70 °C, 12 to 48 h; 4% for **3**; 13% for **29**.

Two macrocyclic products, presumably cis- and trans-isomers, were isolated from the ring-closing metathesis reaction after HPLC purification. One analog, **3a**, was found to have moderate pKal inhibitory activity with an IC_{50} of 1.21 μM; the other isomer **3b** had a similar potency with an IC_{50} of 1.57 μM. Due to the complexity of their proton NMR spectra, unambiguous assignment of the cis- and trans-isomers was not possible. Nevertheless, it seemed that the influence of double-bond geometry on in-vitro enzymatic potency was minimal as suggested by their IC_{50} numbers. However, the macrocyclic analogs, either **3a** or **3b** were much weaker in inhibitory activity compared to the original small molecule **2**. One possible explanation for their poor potency was that the 8-atom linker was too short for efficient binding of **3a** or **3b** to pKal. However, it may also be possible that macrocyclic **3a** or **3b** was forced into a less favorable conformation by the relatively rigid double-bond in their linkers. To rule out this possibility, the double-bond in **3** was hydrogenated to produce the corresponding saturated macrocycle **31** (due to the poor solubility of the free amino compounds, *N*-Boc-protected intermediates were used to synthesize **31**, Supporting Information). The resulting macrocycle **31** with saturated linker was found to be even less potent than either of the two isomers **3a** or **3b** with an IC_{50} of 8.31 μM (**31**), suggesting the rigidity of the double-bond did not affect the enzymatic potency. Together, these results suggested that the linker in these macrocyclic analogs was likely too short to support strong

binding with pKal. Before moving on to synthesize and test macrocycles with longer linkers, we decided to further investigate the aminopyridine group and its orientation in the S1 pocket. As seen in the co-crystal structure (Figures 2&3), the aminopyridine group in the S1 pocket is sandwiched between a group of residues with Cys574 and Cys602 on one side and Trp598 on the other; its pyridine ring was locked in approximately parallel fashion to the indole ring of Trp598. However, due to the poor resolution of the initial X-ray crystal structure (2.3 Å), the exact orientation of the pyridine ring could not be determined based solely on the electron density map. Two possibilities exist: the *N*-atom was facing "up" to solvents or pointing "down" as illustrated in Figure 7. The resolution of the initial co-crystal structures obtained with compound **2** was 2.3 Å, not high enough to distinguish between these two poses. Poorer binding to pKal and negative impact on enzymatic potency would be certainly expected if the aminopyridine group in macrocyclic **3a** and **3b** was forced in an unfavorable conformation by the linker. To address this question, we sought to make compound **32**, a macrocyclic analog with the exact same linker as that in **3** but opposite nitrogen orientation on the pyridine ring (Figure 7).

Figure 7. Two possible orientations of the pyridine ring.

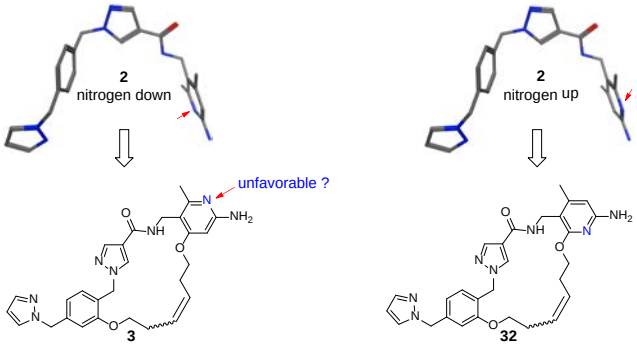

The required *O*-alkenyl aminopyridine derivative **38** was synthesized according to reaction sequence described in Scheme 3. First, commercial cyanopyridine compound **33** was hydrogenated in the presence of boc-anhydride to produce bis-Boc derivative **34**. *O*-alkylation followed by hydrolysis provided acid **36**, which was converted to the corresponding protected *N*-Boc amine **37** through Curtius rearrangement *via* an acyl azide intermediate. Finally, the aminopyridine **38** was obtained after removal of the Boc group under TFA conditions.

Scheme 3. Synthesis of Aminopyridine 38[a]

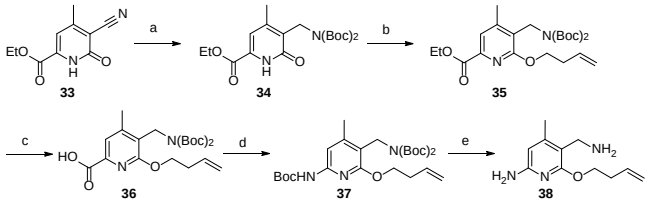

[a]Reagents and conditions: (a) Raney-Ni, H_2, Boc_2O, MeOH, rt, 16 h, 33%; (b) 4-bromobut-1-ene **15**, K_2CO_3, Ag_2CO_3, DMF, 80 °C, 16 h, 50%; (c) NaOH, THF, MeOH, H_2O, 50 °C, 16 h, 77%; (d) TEA, DPPA, *t*-BuOH, toluene, 100 °C, 16 h, 84%; (e) TFA, DCM, rt, 12 h, 98%.

Similar to previous macrocyclic analogs, two versions of (**32**), likely the cis- and trans-isomers, with identical molecular mass were isolated from the reaction mixture (Scheme 4) after HPLC purification. The compounds suffered at least 40-fold potency loss compared to the corresponding macrocycles **3a** and **3b** with IC_{50}s of 53.2 μM for isomer **32a** and IC_{50} > 3 mM for the other isomer **32b**, respectively. Clearly, these results demonstrate the pyridine residue in macrocycle **3** was correctly installed with its ring nitrogen pointing "down". This was confirmed by a high-resolution, 1.7 Å, co-crystal structure of **2** with the protease domain of pKal. As a matter of fact, this nitrogen was involved in a water mediated H-bond with the carboxylate of Asp572 near the bottom of the S1 pocket (Figures 2&3).

Scheme 4. Synthesis of Macrocycle 32[a]

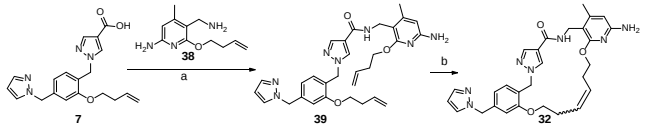

[a]Reagents and conditions: (a) HATU, DIPEA, DMF, rt, 14 h, 52%; (b) Grubbs' catalyst (II), DCE, 70 °C, 48 h, 63%.

With proper resolution of the pyridine ring orientation, we were ready to make macrocycle **29** (Scheme 2), substituting the 8-atom linker with a longer 9-atom linker, aiming to improve binding efficiency and potency. To access this compound we applied a modified synthetic sequence to make the key acid **8** (Scheme 5) as that for macrocycle **3** (Scheme 2). Salicylic acid derivative **19** was transformed, after a series of simple functional groups manipulations, to the phenolic intermediate **46**; the phenol group was *O*-alkylated with a longer 5-bromopent-1-ene **16** to produce the *O*-alkene acid **8**, after hydrolysis of the ester group. Subsequent amide coupling and RCM reaction produced the corresponding macrocycle **29** with a 9-atom linker (Scheme 2, steps i and j).

Scheme 5. Synthesis of Acid 8 for Macrocycle 29[a]

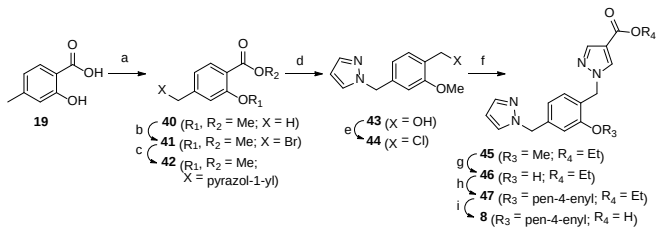

[a]Reagents and conditions: (a) CH_3I, K_2CO_3, DMF, rt, 16 h, 79%; (b) NBS, BPO, CCl_4, 80 °C, 16 h, 100%; (c) pyrazole **22**, K_2CO_3, 50 °C, 16 h, 21%; (d) LAH, THF, 0 - 25 °C, 1 h, 100%; (e) $SOCl_2$, DCM, 0 - 25 °C, 90 min, 100%; (f) ethyl 1H-pyrazole-4-carboxylate **27**, K_2CO_3, DMF, 50 °C, 14 h, 64%; (g) BBr_3, DCM, -78 - 0 °C, 2 h, 52%; (h) 5-bromopent-1-ene **16**, Cs_2CO_3, DMF; 90 °C, 2 h, 66%; (i) NaOH, $MeOH/H_2O$, 50 °C, 85%.

To gain an approximate estimate of its activity, the crude mixture **29** from initial silica gel column purification, containing both cis- and trans-isomers, was assayed directly for pKal activity without separating the two isomers. Consistent with our SAR analysis for longer linkers, **29** was found to be at least 250-fold more potent than compound **3a** or **3b**, having an IC_{50} of 4.8 nM. The mixture was then purified by reverse phase HPLC to separate both isomers. The purified analogs displayed IC_{50} of 2 nM for one olefinic isomer and 42.3 nM for the other, respectively. Once again, unambiguous identification of the cis- and trans-isomers was not possible due to the complex nature of their NMR spectra.

Given the promising potency of **29a** and **29b**, we decided to explore other macrocycles with an isomeric 9-atom linker to evaluate possible influence of double-bond position on their pKal activity (cmpd **30**, Scheme 2 and Table 1). The isomeric

macrocycles were synthesized according to a similar synthetic strategy as outlined in Schemes 1&2 for compound **3**, substituting 4-bromobut-1-ene (**15**) with a longer ω-alkene bromide 5-bromopent-1-ene (**16**) when converting 4-hydroxypyridine **14** to its *O*-alkylated analog **18** (Scheme 1). Compound **30** was obtained after RCM with the bis-alkene intermediate **6** (Scheme 2) (Supporting Information). Compound **30**, tested as a mixture of cis- and trans-isomers, was found to have an IC_{50} of 153 nM, suffering approximately 30-fold potency loss compared to the corresponding isomeric congener (**29**), suggesting that the double bond at this position is less preferred.

To determine if the induced binding conformation by compound **2** was preserved with these macrocycles, several analogs, including **29a**, **29b** and **30**, were selected for co-crystallization experiments using the protease domain of pKal. Unfortunately, except for compound **30**, these analogs failed to yield any co-crystals after several attempts. Interestingly, only the trans-isomer was observed in the co-crystal structure, with a final maximum resolution of 1.4 Å (PDB code 5TJX; Supporting Information). The macrocycle **30** sits in the active site of the protease domain as expected and aligns well when comparing to the structure of the pKal protease domain co-crystallized with compound 2 (Figure 8). The compounds bind in the same orientation and the same key interactions are preserved, this includes hydrogen bonds to the sidechain of Asp572 and carbonyl of Ser597. There are however subtle differences stemming from the addition of a large linker to connect the aminopyridine and the phenyl group. The phenyl group appears shifted out of plane when compared to compound **2**. This likely results in the shift of the S4 pyrazole and the second pyrazole shown to form a pi-pi stacking interaction with His434. Compared to the in-silico modeling, compound **30** aligns well in the S1 pocket but changes drastically after exiting the S1 pocket (Figure 8). By aligning the two molecules we calculate an overall RMSD of approximately 0.763 Å between the in-silico model and crystallographic model, with a majority of differences coming from arrangement of the linker.

Figure 8. Comparison of **2**, macrocycle **30** (co-crystal and in-silico model generated using MOE). Numbers in parenthesis represent the canonical chymotrypsin numbering scheme. Two water molecules are shown as blue spheres.

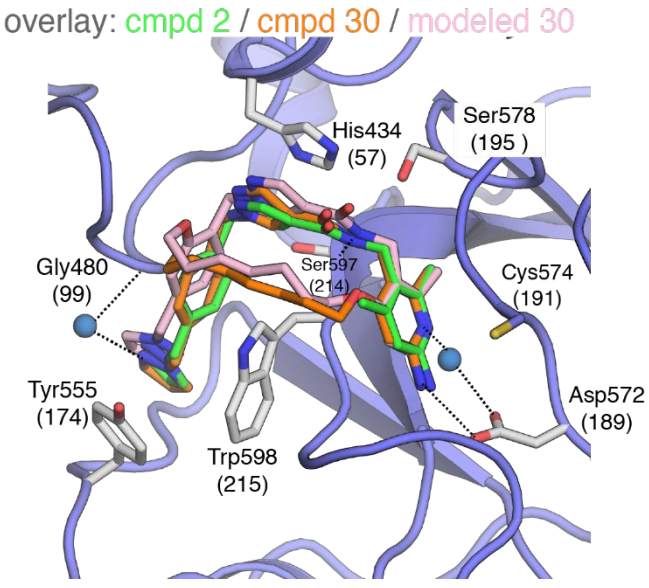

Next, the most active macrocyclic compounds **29a**, **29b**, **29** and **30**, along with compound **2** were profiled in a protease panel containing eight closely-related proteases to evaluate their selectivity profiles. All four macrocycles displayed excellent selectivity similar to that seen with the precursor molecule **2** (Table 2). These results were not unexpected since the induced binding conformation, the origin of good selectivity, was preserved with the macrocyclic analogs. These macrocyclic analogs had little effects (IC50 > 200 μM) on the enzymatic activities of several proteases including plasmin, trypsin, TPA, thrombin, FXa, and FXIIa; and even though these compounds inhibited the activity of FXIa with moderate IC_{50}s ranging from single-digit to double-digit micromolar (Table 2), these activities were at least 1,800-fold less potent compared to the IC_{50}s for pKal.

Table 1. Plasma kallikrein potency for 2 and macrocycles.

Cmpd	pKal IC_{50} (nM)	N (Tests performed)
2	2.4 ± 1.1	82
3a	(1.21 ± 0.040) x10^3	4
3b	(1.57 ± 0.58) x10^3	4
29	4.8 ± 1.8	6
29a	2.0 ± 0.0	3
29b	42.3 ± 12	4
30	153 ± 14.1	5
31	(8.31 ± 2.28) x10^3	3
32a	(53.2 ± 2.8) x10^3	3
32b	inactive	3

Table 2. Inhibitory activities of 2 and macrocycles against eight proteases.

Cmpd	2	29	29a	29b	30
pKal IC_{50} (μM)	2.4 x10^{-3}	4.8 x10^{-3}	2.0 x10^{-3}	42.3 x10^{-3}	153 x10^{-3}
Plasmin IC_{50} (μM)	> 10^3	21.4±4.1	> 200	> 200	9.97± 3.86
fXa IC_{50} (μM)	> 10^3	> 200	> 200	> 200	> 200
fXIa IC_{50} (μM)	106	11.7 ± 0.3	3.61±1.79	40.9±2.8	12.7± 0.54
fXIIa IC_{50} (μM)	> 10^3	> 200	> 200	> 200	> 200
Trypsin IC_{50} (μM)	578	> 200	> 200	> 200	> 200
tPA IC_{50} (μM)	> 10^3	> 200	> 200	> 200	> 200
Thrombin IC_{50} (μM)	> 10^3	> 200	> 200	> 200	> 200

In-vivo rat pharmacokinetic (PK) studies on the most active compounds in the series were performed to evaluate PK profiles and assess their potential as possible drug leads. Instead of dosing each isomer, the mixtures **29** and **30** containing both the cis- and trans-isomers were administered in rat by oral gavage to gain quick readouts on their oral exposure. Unfortunately, both compounds displayed little or no exposure. To better understand the PK results, microsomal stability and permeability were measured for these compounds. All four analogs were found to have poor permeability with their P_{app} numbers well below 1 cm^{-6}/s (Supporting Information). More surprisingly, all four compounds displayed extremely short half-life (< 5 min; comparing to 48 min for **2**) and were metabolized rapidly by rat

liver microsomal isolates in vitro. Due to these poor properties, further work on the macrocycles were terminated.

In summary, novel macrocyclic plasma pKal inhibitors were designed based on the co-crystal structure of pKal with small molecule pKal inhibitor **2**. Guided by structure information and modeling tool, we discovered a series of potent macrocyclic pKal inhibitors, typified by **29a**, having low nanomolar activity (2.0 nM), after two rounds of linker optimization. Importantly, these novel macrocyclic analogs retained the unique binding conformation and excellent selectivity for a group of closely related proteases. The work demonstrated the power and utility of SBDD in aiding the design of novel enzyme inhibitors in drug discovery project.

ASSOCIATED CONTENT.

Supporting Information. Experimental details and analytical data for all macrocycles and synthetic intermediates, in vitro and in vivo biological procedures, as well as modeling and crystallographic methods. This material is available free of charge via the internet at http://pubs.acs.org.

AUTHOR INFORMATION.

Corresponding Author

* E-mail: zli@globalbloodtx.com

Present Addresses

Andreas Betz: abetz@allostery.com

Notes. The authors declare the following competing financial interest(s): The authors ZL, JP, AS, PR, AB, QX and HS are, employees of Global Blood Therapeutics which has a commercial interest in pKal inhibitors.

ACKNOWLEDGMENT. The authors thank Drs. Manuel Zancanella and Shahul Nilar for reviewing the manuscript. We thank J. Holton, G. Meigs and ALS staff of beamline 8.3.1 for data collection and helpful discussions. Beamline 8.3.1 at the Advanced Light Source is operated by the University of California Office of the President, Multicampus Research Programs and Initiatives grant MR-15-328599 and Program for Breakthrough Biomedical Research, which is partially funded by the Sandler Foundation. Additional support comes from National Institutes of Health (GM105404, GM073210, GM082250, GM094625), National Science Foundation (1330685), Plexxikon Inc. and the M.D. Anderson Cancer Center. The Advanced Light Source (Berkeley, CA), a national user facility operated by Lawrence Berkeley National Laboratory on behalf of the US Department of Energy under contract number DE-AC02-05CH11231, Office of Basic Energy Sciences, through the Integrated Diffraction Analysis Technologies program, supported by the US Department of Energy Office of Biological and Environmental Research.

ABBREVIATIONS. BPO, benzoyl peroxide; DIPEA, *N*,*N*-diisopropylethylamine; DPPA, Diphenylphosphoryl azide; fXa, factor Xa; fXIa, factor XIa; fXIIa, factor XIIa; HAE, hereditary angioedema; HATU, 2-(1H-7-azabenzotriazol-1-yl)-1,1,3,3-tetramethyluronium hexafluorophosphate; pKal, plasma kallikrein; RCM, ring-closing metathesis; tPA, tissue plasminoogen activator.

REFERENCES

(1) Bryant, J.W.; Shariat-Madar, Z. Human plasma kallikrein kinin system: physiological and biochemical parameters. Cardiovasc. Hematol. Agents Med. Chem. **2009**, *7*, 234-50.

(2) Kaplan, A. P. Bradykinin and the Pathogenesis of Hereditary Angioedema. World Allergy Organ J. **2011**, *4*, 73-75.

(3) Maas, C.; Oschatz, C.; Renne, T. The plasma contact system 2.0. Semin. Thromb. Hemost. **2011**, *37*, 375-38.

(4) Levy, J.H.; Freiberger, D.J.; Roback, J. Hereditary angioedema: current and emerging treatment options. Anesthesia & Analgesia **2010**, *110*, 1271-1280.

(5) Schneider, L.; Lumry, W.; Vegh, A.; Williams, A.H.; Schmalbach, T. Critical role of kallikrein in hereditary angioedema pathogenesis: a clinical trial of escallantide, a novel kallikrein inhibitor. J. Allergy Clin. Immunol. **2007**, *120*, 416-422.

(6) Chyung, Y.; Vince, B.; Iarrobino, B.; Sexton, D.; Kenniston, J.; Faucette, R.; TenHoor, C.; Stolz, L.E.; Stevens, C.; Biedenkapp, J.; Adelman, B. A phase 1 study investigating DX-2930 in healthy subjects. Annals of Allergy, Asthma & Immunology **2014**, *113*, 460-466.

(7) Aygören-Pürsün, E.; Magerl, M.; Graff, J.; Martinez-Saguer, I.; Kreuz, W.; Longhurst, H.; Nasr, I.; Bas, M.; Straßen, U.; Fang, L.; Cornpropst, M.; Dobo, S.; Collis, P.; Sheridan, W.P.; Maurer, M. Prophylaxis of hereditary angioedema attacks: A randomized trial of oral plasma kallikrein inhibition with avoralstat. J Allergy Clin Immunol. **2016**, pii: *S0091-6749*, 30270-30276.

(8) Cornpropst, M.; Dobo, S.; Collier, J.; Rose, A.; Wilson, R.; Babu, Y.S.; Collis, P.; Zong, J.; Sheridan, W.P. BCX7353, a Potent Inhibitor of Plasma Kallikrein, Shows Sustained Maximal Enzyme Inhibition when Dosed Orally Once Daily: Results from a Phase I Trial in Healthy Subjects. AAAAI Annual Meeting, March 3-8, **2016**, Los Angeles, CA.

(9) Brandl, T.; Flohr, S.; Kopec, S.; Lachal, J.; Merkert, C.; Namoto, K.; Nganga, P.; Pirard, B.; Renatus, M.; Sedrani, R.; Zoller, T. N-((6-amino-pyridin-3-yl)methyl)-heteroaryl-carboxamides as inhibitors of plasma kallikrein. WO2012017020A1, February 12, **2012**.

(10) Partridge, J.; Choy, R., Li, Z. Manuscript in preparation.

(11) Kobayashi,T.; Suemasa,A.; Igawa, A.; Ide,S.; Fukuda,H.; Abe, H.; Arisawa, M.; Minami, M.; Shuto, S. Conformationally Restricted GABA with Bicyclo[3.1.0]hexane Backbone as the First Highly Selective BGT‑1 Inhibitor. ACS Med. Chem. Lett. **2014**, *5*, 889−893.

(12) Spear, K.L.; Brown, M.S.; Reinhard, M.J.; McMahon, E.G.; Olins, G.M.; Palomo, M.A.; Patton, D. R. Conformational Restriction of Angiotensin II: Cyclic Analogues Having High Potency. J. Med. Chem. **1990,** *33*, 1935-1940.

(13) Bakali, J.E.; Muccioli, G.G.; Body-Malapel, M.; Djouina, M.; Klupsch, F.; Ghinet, A.; Barczyk, A.; Renault,N.; Chavatte, P.; Desreumaux, P.; Lambert, D.M.; Millet, R. Conformational Restriction Leading to a Selective CB2 Cannabinoid Receptor Agonist Orally Active Against Colitis. ACS Med. Chem. Lett. **2015**, *6*, 198−203.

(14) Molecular Operating Environment (MOE), 2014.09; Chemical Computing Group Inc., 1010 Sherbooke St. West, Suite #910, Montreal, QC, Canada, H3A 2R7, 2014.

(15) Fu, G. C.; Grubbs, R. H. The Application of Catalytic Ring-Closing Olefin Metathesis to the Synthesis of Unsaturated Oxygen Heterocycles. J. Am. Chem. Soc. **1992**, *114*, 5426-5427.

(16) Fu, G. C.; Grubbs, R. H. Synthesis of Nitrogen Heterocycles via Catalytic Ring Closing Metathesis of Dienes. J. Am. Chem. Soc. **1992**, *114*, 7324-7325.

(17) Scholl, M.; Ding, S.; Lee, C. W.; Grubbs, R. H. Synthesis and Activity of a New Generation of Ruthenium-Based Olefin Metathesis Catalysts Coordinated with 1,3-Dimesityl-4,5-dihydroimidazol-2-ylidene Ligands. Org. Lett. **1999**, *6*, 953–956.

For Table of Contents Use Only

Structure-Guided Design of Novel, Potent and Selective Macrocyclic Plasma Kallikrein Inhibitors

Zhe Li,[†,*] James Partridge,[†] Abel Silva,[†] Peter Rademacher,[†] Andreas Betz,[†] Qing Xu,[†] Hing Sham,[†] Yunjin Hu,[‡] Yuqing Shan,[‡] Bin Liu,[‡] Ying Zhang,[‡] Haijuan Shi,[‡] Qiong Xu,[‡] Xubo Ma,[‡] Li Zhang[‡]

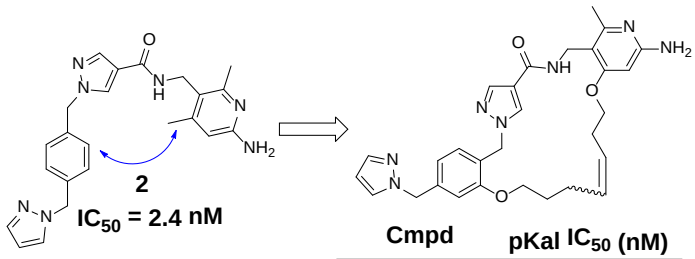

Cmpd	pKal IC_{50} (nM)
29a-isomer 1	**2**
29b-isomer 2	**42.3**